Perturbation solution for spherical and cylindrical solidification by combined convective and radiative cooling

M. Parang, D. S. Crocker, and B. D. Haynes
Mechanical and Aerospace Engineering Department, University of Tennessee, Knoxville, TN, USA

The problem of inward solidification of a liquid in cylindrical and spherical geometries is considered. Freezing is accomplished at the boundary by both radiative and convective cooling. The liquid is assumed at its melt temperature. The method of strained coordinates is used and the zeroth and first-order solutions are developed for freezing-front location, total freezing time, and temperature profile in the solid. The results are compared with a numerical solution, obtained by using the enthalpy method, for various values of the Stefan number. There is excellent agreement between the solutions for small Stefan number. The advantages of the perturbation method (simplicity, relatively good accuracy) in certain cases are discussed and elaborated.

Keywords: heat transfer; solidification; radiative–convective cooling; perturbation method

Introduction

The problem of heat conduction through a medium with phase change has been the subject of numerous studies. The phase change problems in such practically important geometries as spheres and cylinders have no exact solutions except in very simple and special cases. These geometries have various applications in aerodynamic heating of spaceships and reactor fuel elements (melting) and groundwater freezing and casting of metals (solidification). There are no exact solutions for bounded spherical or cylindrical regions. Therefore a large number of studies have been devoted to the development of approximate solutions to this and similar classes of problems. Extensive lists of references can be found in Wilson *et al.*,[1] Rubinstein,[2] Crank,[3] and Ockendon and Hodgkins.[4] An interesting and useful mathematical tool is the perturbation method,[5–7] which has been used effectively in this and similar classes of problems.[8–16] The perturbation method can, in this case, provide a simple and fast method of solution without a significant loss of accuracy.

A regular parameter perturbation technique was applied to the problem of outward and inward solidification in radial systems by Huang and Shih.[17] They showed that, although the regular parameter expansion gives accurate solutions for the outward solidification problem, the scheme fails for inward freezing in the radial systems owing to singularities near the center. After finding similar results using regular perturbation expansions, Pedroso and Domoto[18] successfully developed uniformly valid solutions by applying the method of strained coordinates for the inward solidification in spheres at constant wall temperature. Using the same method, Milanez and Boldrini[19] discussed and solved the more complicated problem of inward solidification in spheres with convective wall condition.

The focus of the present study is the problem of inward solidification in spheres and cylinders with combined convective and radiative cooling at the wall. The contribution of radiation in solidification problems is determined by numerical solution of the governing equations[20] and discussed. The presence of significant radiative cooling at the boundary of radial systems may be encountered in space solidification processes. Also, natural convection and radiative cooling may be both significant in cooling with phase change problems in microgravity when, for example, electromagnetic levitation furnaces or acoustic levitators are used. For a small Stefan number, the method of strained coordinates[18,19] is used to obtain the solution for temperature and total freezing time. Mathematically the problem involves two additional complexities: (1) the nonlinear radiative boundary condition imposed at the wall; and (2) the existence of an additional parameter indicating the relative importance of radiative to convective contributions in the solidification process.

Following solution of the problem by the method of strained coordinates, the accuracy and effectiveness of the perturbation analysis is then compared with the numerical solution of the equations governing the inward solidification of a liquid at its fusion temperature in both spheres and cylinders. The numerical method selected for this purpose is the enthalpy method. A detailed discussion of the method can be found in various references, including Voller and Cross[21] and Voller.[22]

Address reprint requests to Professor Parang, Mechanical and Aerospace Engineering Department, University of Tennessee, Knoxville, TN 37996, USA.

Received 11 March 1989; accepted 24 October 1989

Analysis

Perturbation

Consider a radial system (a sphere or cylinder) with radius R_o containing a fluid with constant properties at its freezing temperature T_f. The system is suddenly cooled by convection and radiation through exposure to a medium at T_∞ with an average heat transfer coefficient h. A schematic of the problem configuration is shown in Figure 1. The governing equations for solidification and the corresponding initial and boundary conditions are

$$\frac{\partial T}{\partial t}=\frac{K}{\rho CR}\frac{\partial}{\partial R}\left[R\frac{\partial T}{\partial R}\right]+j\frac{K}{\rho CR}\frac{\partial T}{\partial R} \qquad R_f\le R\le R_o \tag{1}$$

where j is 0 (cylinder) or 1 (sphere). The boundary conditions

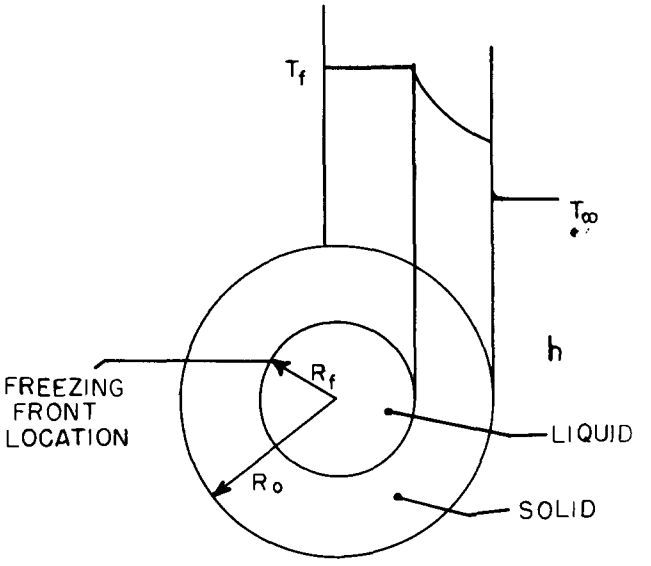

Figure 1 Sphere or cylinder cross section with radial temperature profile

are

$$T(t, R<R_f)=T_f \tag{2}$$

$$-K\frac{\partial T}{\partial R}=h(T-T_\infty)+\sigma e(T^4-T_\infty^4) \qquad R=R_o \tag{3}$$

$$\rho L\frac{\partial R_f}{\partial t}=K\frac{\partial T}{\partial R} \qquad R=R_f \tag{4}$$

The following nondimensional variables are introduced:

$$r=\frac{R}{R_o}, \quad r_f=\frac{R_f}{R_o}, \quad \theta=\frac{T}{T_f}, \quad \alpha=\frac{T_\infty}{T_f}, \quad \mathrm{Bi}=\frac{hR_o}{K}$$
$$\mathrm{Bi}_r=\frac{\sigma e T_f^3 R_o}{K}, \quad \varepsilon=\frac{CT_f}{L}, \quad \tau=\frac{KT_f t}{\rho L R_o^2}, \quad \beta=\frac{Bi}{Bi_r}=\frac{h}{\sigma e T_f^3} \tag{5}$$

where Bi and Bi_r are the Biot number and equivalent radiation "Biot" number, respectively, ε is equivalent to the Stefan number based on the absolute freezing temperature, and τ is dimensionless time. Substituting Equation 5 into Equations 1–4 yields the following system of equations:

$$\varepsilon\frac{\partial\theta}{\partial r_f}\frac{\partial\theta}{\partial r}\bigg|_{r=r_f}=\frac{1}{r}\frac{\partial}{\partial r}\left(r\frac{\partial\theta}{\partial r}\right)+j\frac{1}{r}\frac{\partial\theta}{\partial r} \qquad r_f<r<1 \tag{6}$$

$$\theta(r_f, r=r_f)=1 \tag{7}$$

$$-\frac{1}{\mathrm{Bi}_r}\frac{\partial\theta}{\partial r}=\beta(\theta-\alpha)+(\theta^4-\alpha^4) \qquad r=1 \tag{8}$$

$$\frac{\partial r_f}{\partial\tau}=\frac{\partial\theta}{\partial r}\bigg|_{r=r_f} \tag{9}$$

We now solve these equations by applying the method of strained coordinates. The two coordinates chosen for straining are r and r_f:

$$r=\Phi+\sum_{i=1}^{\infty}\varepsilon^i\sigma_i(\Psi, \Phi) \tag{10}$$

$$r_f=\Psi+\sum_{i=1}^{\infty}\varepsilon^i\sigma_i(\Psi, \Phi=\Psi) \tag{11}$$

where $\sigma_i(\Psi, \Phi)$ will be determined as part of the solution of the problem. We further assume that

$$\lim_{\Phi\to 1}\sigma_i(\Psi, \Phi)=\lim_{\Psi\to 1}\sigma_i(\Psi, \Psi)=0$$

so that the boundary conditions at the wall and at the initial position of freezing front are satisfied.

Expanding the dependent variable, temperature, in terms of the strained coordinates gives

$$\theta=\theta_o+\sum_{i=1}^{\infty}\varepsilon^i\theta_i(\Psi, \Phi) \tag{12}$$

We now change the independent variables in the system of Equations 6–9 from (r, r_f) to (Φ, Ψ). We then expand these equations in terms of ε to obtain the zeroth- and first-order equations.

The zeroth-order equations are:

$$\frac{\partial}{\partial\Phi}\left[\Phi\frac{\partial\theta_o}{\partial\Phi}\right]+j\frac{\partial\theta_o}{\partial\Phi}=0 \tag{13}$$

$$\theta_o(\Psi, \Phi=\Psi)=1 \tag{14}$$

$$-\frac{1}{\mathrm{Bi}_r}\frac{\partial\theta_o}{\partial\Phi}=\beta(\theta_o-\alpha)+(\theta_o^4-\alpha^4) \qquad \Phi=1 \tag{15}$$

Notation

Bi	Biot number
Bi_r	Equivalent radiation Biot number
C	Heat capacity of solid
C_1, C_2	Integration constants
e	Emissivity of the boundary
h	Convection heat transfer coefficient
H	Dimensionless enthalpy
H_d	Enthalpy (latent and sensible)
j	0 for the cylinder; 1 for the sphere case
K	Thermal conductivity of solid
L	Latent heat of fusion
r	Dimensionless radial position
r_f	Dimensionless radial position of the freezing front
R	Radial position
R_f	Radial position of the freezing front
R_o	Radius of the sphere or cylinder
t	Time
T	Temperature in solid
T_f	Freezing temperature
T_∞	Temperature of the cooling environment

Greek symbols

α	Dimensionless ambient temperature, T_∞/T_f
β	Ratio of convection to radiation Biot numbers, $\mathrm{Bi}/\mathrm{Bi}_r$
ε	Stefan number, CT_f/L
θ	Dimensionless temperature in solid
ρ	Density of solid
σ	Stefan–Boltzmann constant
σ_i	Straining variable
τ	Dimensionless time
Φ	Straining function
Ψ	Straining function

The first-order equations are:

$$\Phi\frac{\partial^2\theta_1}{\partial\Phi^2}+(1+j)\frac{\partial\sigma_1}{\partial\Phi}\frac{\partial\theta_o}{\partial\Phi}-\Phi\frac{\partial^2\sigma_1}{\partial\Phi^2}\frac{\partial\theta_o}{\partial\Phi}+\sigma_1\frac{\partial^2\theta_o}{\partial\phi^2}+(1+j)\frac{\partial\theta_1}{\partial\Phi}$$

$$=\Phi\frac{\partial\theta_o}{\partial\Psi}\frac{\partial\theta_o}{\partial\Phi}\bigg|_{\Phi=\Psi} \tag{16}$$

$$\theta_1(\Psi,\Phi=\Psi)=0 \tag{17}$$

$$\theta_1=\frac{-\left[\dfrac{\partial\theta_1}{\partial\Phi}-\dfrac{\partial\sigma_1}{\partial\Phi}\dfrac{\partial\theta_o}{\partial\Phi}\right]}{\mathrm{Bi}_r[4\theta_o^3+\beta]}\qquad\Phi=1 \tag{18}$$

Solving the zeroth-order equations for the sphere gives

$$\theta_o=\frac{C_2}{\Phi}+C_1 \tag{19}$$

where the coefficients $C_1(\Phi,\Psi)$ and $C_2(\Phi,\Psi)$ are obtained from the following equations by applying the boundary conditions:

$$C_2=\Psi(1-C_1) \tag{20}$$

$$C_1^4+\frac{4\Psi}{(1-\Psi)}C_1^3+\frac{6\Psi^2}{(1-\Psi)^2}C_1^2+\left[\frac{4\Psi^3+\beta}{(1-\Psi)^3}+\frac{\Psi}{\mathrm{Bi}_r(1-\Psi)^4}\right]C_1$$

$$+\frac{\Psi^4-\alpha^4+\beta(\Psi-\alpha)-(\Psi/\mathrm{Bi}_r)}{(1-\Psi)^4}=0 \tag{21}$$

Similarly, for the cylinder:

$$\theta_o=C_1\ln\Phi+C_2 \tag{22}$$

with the coefficients again found by applying the boundary conditions:

$$C_2=1-C_1\ln\Psi \tag{23}$$

$$C_1^4-\frac{4C_1^3}{\ln\Psi}+\frac{6C_1^2}{(\ln\Psi)^2}-\frac{C_1(4+\beta)}{(\ln\Psi)^3}+\frac{(1-\alpha^4+\beta(1-\alpha)+C_1/\mathrm{Bi}_r)}{(\ln\Psi)^4}=0 \tag{24}$$

Equations 21 and 24 are implicit polynomials for the constant C_1. Although their solution is trivial and only requires a simple numerical scheme to find the roots, they prevent the casting of the solution of $\theta_0(\Phi,\Psi)$ and $\theta_1(\Phi,\Psi)$ *in an explicit form*. We now choose the straining function, σ_1, so that the first-order term in the temperature expansion, θ_1, is identically zero. This choice provides a differential equation for the function $\sigma_1(\Phi,\Psi)$:

$$\Phi^2\frac{\partial^2\sigma_1}{\partial\Phi^2}-(1+j)\Phi\frac{\partial\sigma_1}{\partial\Phi}+(1+j)\sigma_1$$

$$=-\frac{\Phi^3}{\Psi^{1+j}}\left[(1-j)\ln(\Phi)\frac{dC_1}{d\Psi}+j\Phi\frac{dC_1}{d\Psi}+\frac{dC_2}{d\Psi}\right] \tag{25}$$

with boundary conditions

$$\sigma_1(\Psi,\Phi=1)=0 \tag{26}$$

$$\frac{\partial\sigma_1}{\partial\Psi}(\Psi,\Phi=1)=0 \tag{27}$$

Equations 25–27 are forced Euler equations. The solution for the sphere is

$$\sigma_1=-\frac{1}{\Psi^2}\left[\frac{1}{6}\frac{dC_1}{d\Psi}\Phi^4+\frac{1}{2}\frac{dC_2}{d\Psi}\Phi^3-\frac{1}{2}\left(\frac{dC_1}{d\Psi}+2\frac{dC_2}{d\Psi}\right)\Phi^2\right.$$

$$\left.+\frac{1}{6}\left(2\frac{dC_1}{d\Psi}+3\frac{dC_2}{d\Psi}\right)\Phi\right] \tag{28}$$

and for the cylinder is

$$\sigma_1=\frac{1}{4\Psi}\left\{\left[\frac{dC_2}{d\Psi}-\frac{dC_1}{d\Psi}+\left(2\frac{dC_2}{d\Psi}-\frac{dC_1}{d\Psi}\right)\ln\Phi\right]\Phi\right.$$

$$\left.+\left(\frac{dC_1}{d\Psi}-\frac{dC_2}{d\Psi}-\frac{dC_1}{d\Psi}\ln\Phi\right)\Phi^3\right\} \tag{29}$$

We use Equations 19–24, 28, and 29 to calculate the freezing front location and the freezing time of the enclosed fluid for various values of the parameters ε, α, and β.

We obtain the total freezing time by using an energy balance at the freezing front (Equation 9) and

$$\frac{d\tau}{d\Psi}=\frac{d\tau}{dr_f}\frac{dr_f}{d\Psi} \tag{30}$$

to give

$$\frac{d\tau}{d\Psi}=\frac{dr_f}{d\Psi}\left(\frac{\partial\theta_o}{\partial\Phi}\frac{\partial\Phi}{\partial r}\right)^{-1}\bigg|_{\Phi=\Psi} \tag{31}$$

with the initial condition

$$\tau(\Psi=1)=0 \tag{32}$$

Substituting Equations 19, 20, 21, and 28 (for the sphere) and Equations 22, 23, 24, and 29 (for the cylinder) into Equation 31 provides the total freezing time for the various values of parameters ε, α, and β.

Numerical solution

In order to evaluate the results of the perturbation analysis, we compare them with the numerical solution of the governing equations for freezing of radial systems described by Equations 1–4. For this purpose we cast the equations in terms of enthalpy H_d (sum of latent and sensible heats).[21,22] If we define nondimensional enthalpy as

$$H=\frac{H_d}{CT_f}$$

the energy equation and boundary condition become

$$\frac{\partial H}{\partial\tau}=\frac{1}{\varepsilon}\frac{1}{r}\frac{\partial}{\partial r}\left(r\frac{\partial\theta}{\partial r}\right)+j\frac{1}{r}\frac{\partial\theta}{\partial r} \tag{33}$$

$$\frac{\partial\theta}{\partial r}\bigg|_{r=1}=-\mathrm{Bi}(\theta-\alpha)-\mathrm{Bi}_r(\theta^4-\alpha^4) \tag{34}$$

where temperature and enthalpy are related by

$$\theta=\begin{cases}H & H\le 1\\ 1 & 1<H<1+1/\varepsilon\\ H-\dfrac{1}{\varepsilon} & H\ge 1+1/\varepsilon\end{cases} \tag{35}$$

Furthermore, for the center node we impose the condition:

$$\lim_{r\to 0}\frac{1}{r}\frac{\partial\theta}{\partial r}=\frac{\partial^2\theta}{\partial r^2}=0 \tag{36}$$

We solve Equations 34–36 for both enthalpy and temperature, using a finite difference formulation similar to that presented in ref. 17. We calculate the position of the front at any particular time by using a volume-weighted interpolation in space between the appropriate consecutive nodes where the front is located.

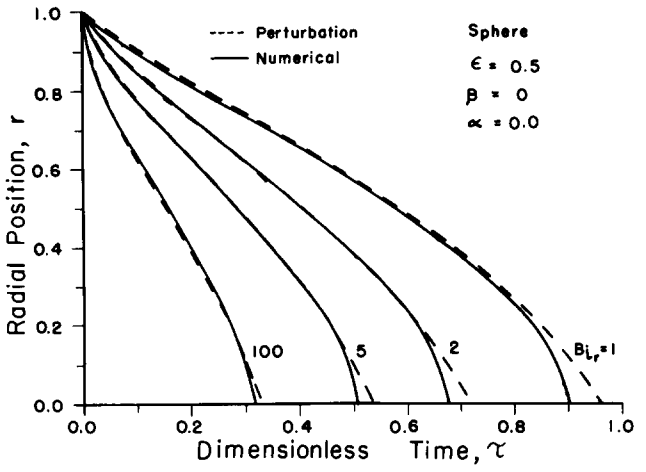

Figure 2 Freezing front location as a function of time for various Bi_r (sphere: $\beta=0$)

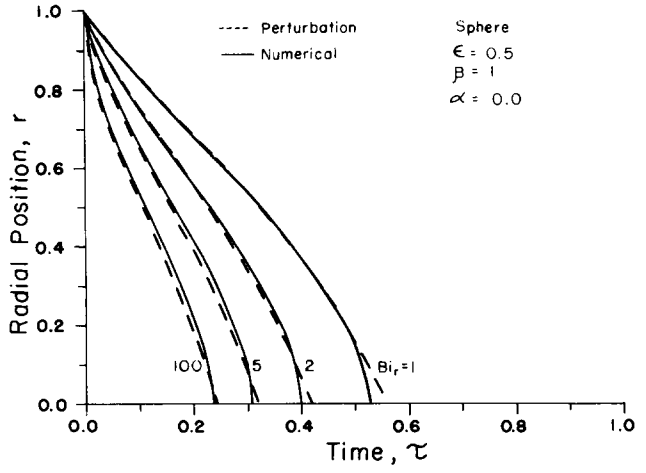

Figure 3 Freezing front location as a function of time for various Bi_r (sphere: $\beta=1$)

Results and discussion

Freezing front location

The freezing front position and its movement in the enclosed fluid is found by perturbation method and compared with the results of the numerical analysis. For this purpose the front location as a function of time is presented in Figures 2–4 for the sphere. The dimensionless ambient temperature, α, is zero in these figures. The Stefan number, ε, is 0.5. Figure 2 illustrates the location of the front at different times for no convection at the surface ($\beta=0.0$) at various radiative cooling rates (Bi_r from 1 to 100). Figure 3 shows the results for the same range of Biot number but for equal convective and radiative contributions ($\beta=1.0$). The perturbation and numerical results in this case are also tabulated for comparison purposes in Table 1. Finally,

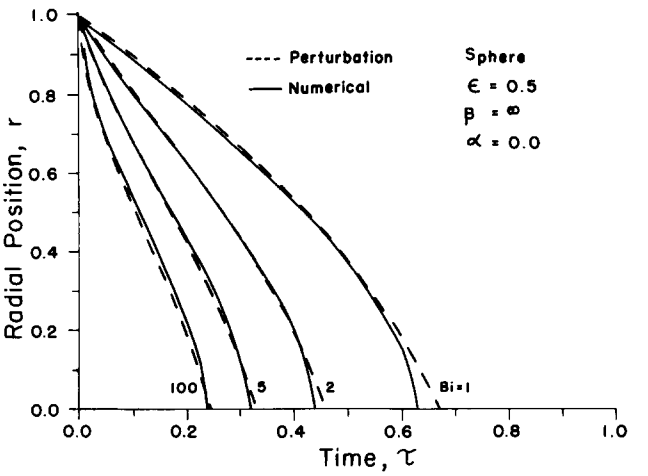

Figure 4 Freezing front location as a function of time for various Bi_r (sphere: $\beta=\infty$)

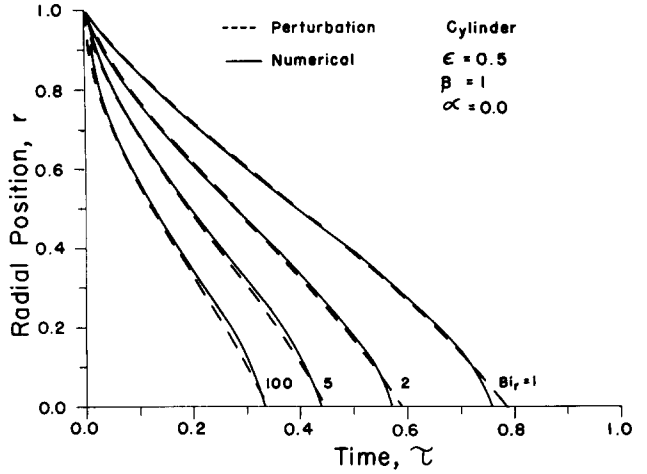

Figure 5 Freezing front location as a function of time for various Bi_r (cylinder: $\varepsilon=0.5$)

Figure 4 presents the location of the front in the absence of radiation at the surface of the sphere ($\beta=\infty$). For the entire range of the Biot numbers discussed, the perturbation results are in very good agreement with the numerical results at this value of the Stefan number. The divergence of the two results is slightly more pronounced near the center of the sphere but still remains small (less than 7%). Comparison of Figures 2 and 4 also suggests that, for a given value of the Biot number, pure convective cooling ($\beta=\infty$) is more effective than pure radiative cooling ($\beta=0$) at zero dimensionless temperature. That is, the total freezing time for $\beta=\infty$ is, depending on Biot number, only about half the time needed for $\beta=0$.

The effect of varying the Stefan number is illustrated for the case of cylinder in Figures 5–7. The dimensionless temperature

Table 1 Required freezing time calculated by the perturbation and numerical methods for different Bi_r (sphere: $\varepsilon=0.5$, $\beta=1.0$, $\alpha=0.0$)

r	0.0		0.2		0.4		0.6		0.8	
Bi_r	Num.	Pert.	Num.	Pert.	Num.	Pert.	Num.	Pert.	Num.	Pert.
1	.52150	.5554	.47664	.48034	.38146	.38184	.25602	.25956	.11774	.12348
2	.39450	.4163	.35544	.35384	.27612	.27300	.17709	.17736	.07537	.07811
5	.30300	.3164	.26812	.26360	.20055	.19561	.12114	.11949	.04650	.04755
100	.23060	.2390	.19835	.19311	.13842	.13400	.07365	.07191	.02242	.02181

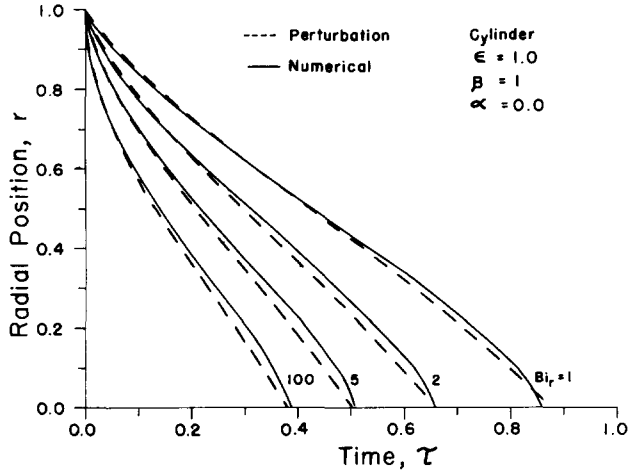

Figure 6 Freezing front location as a function of time for various Bi_r (cylinder: $\varepsilon=1.0$)

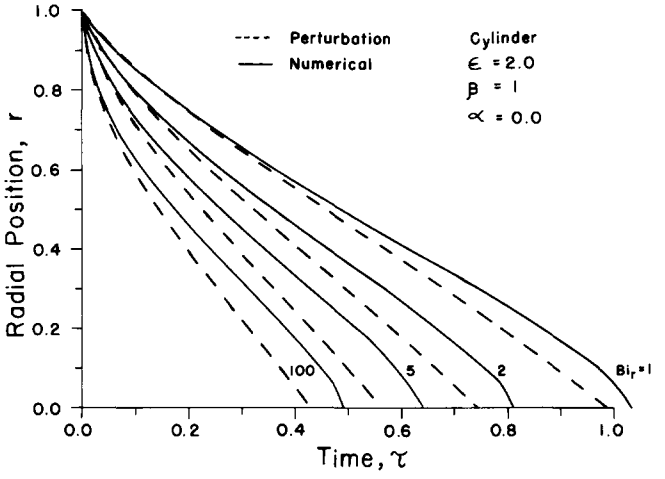

Figure 7 Freezing front location as a function of time for various Bi_r (cylinder: $\varepsilon=2.0$)

is selected to be zero and the relative effects of convective and radiative cooling are set equal ($\beta=1.0$). Figure 5 shows the results for $\varepsilon=0.5$, Figure 6 for $\varepsilon=1.0$, and Figure 7 for $\varepsilon=2.0$. For $\varepsilon=0.5$, the perturbation and numerical results are also presented and compared in Table 2. The divergence of the two results increases with increases in the value of the Stefan number, as expected. However, even for $\varepsilon=1.0$, the difference in the results is still small and remains below 10% for all values of the Biot number. For $\varepsilon=2.0$, the divergence reaches a maximum of about 18%. Comparison of Figure 3 and Figure 5 shows that the freezing time for a cylinder is considerably larger than for a sphere of the same radius.

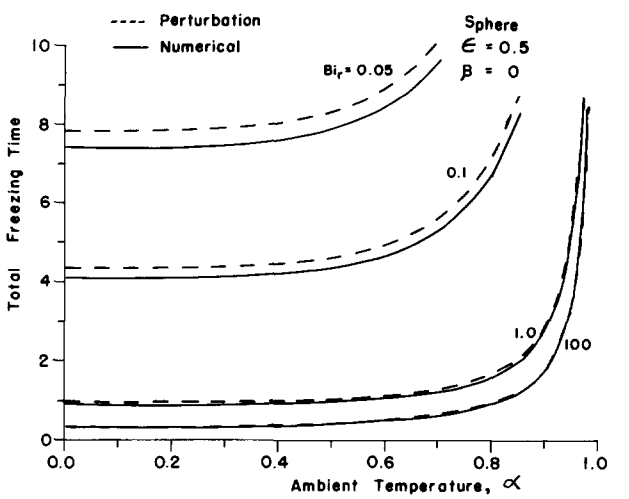

Figure 8 Time for complete freezing as a function of ambient temperature for various Bi_r (sphere: $\beta=0$)

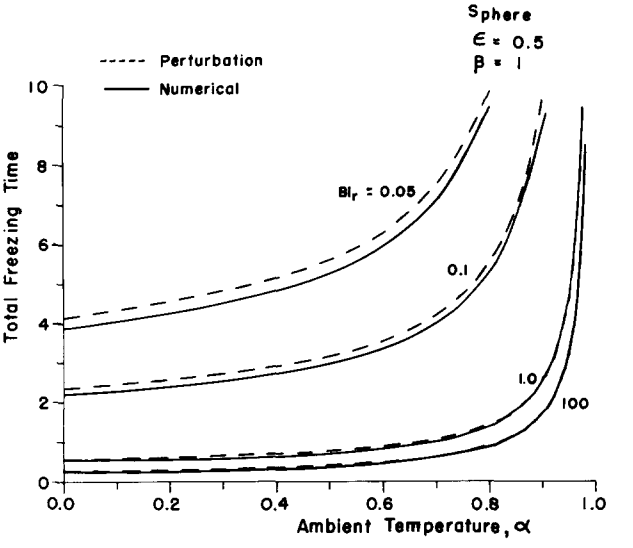

Figure 9 Time for complete freezing as a function of ambient temperature for various Bi_r (sphere: $\beta=1$)

Total freezing time

The effect of variation of the dimensionless ambient temperature on the total required freezing time of the enclosed liquid is presented in Figures 8, 9, and 10 for $\varepsilon=0.5$ and $\beta=0$, 1, and ∞, respectively. The range selected for the appropriate Biot number in each case is 0.05 to 100. Comparison of Figures 8 and 10 indicates that convective cooling is more effective than radiative cooling at smaller values of α (e.g., $\alpha<0.3$ for $Bi_r=1.0$, and $\alpha<0.2$ for $Bi_r=0.1$), but the inverse is true for large α and

Table 2 Required freezing time calculated by the perturbation and numerical methods for different Bi_r (cylinder: $\varepsilon=0.5$, $\beta=1.0$, $\alpha=0.0$)

r	0		0.2		0.4		0.6		0.8	
Bi_r	Num.	Pert.	Num.	Pert.	Num.	Pert.	Num.	Pert.	Num.	Pert.
1	.75250	.7847	.65375	.65340	.48740	.48825	.30341	.30756	.12885	.13483
2	.56600	.5869	.48323	.47843	.34951	.34662	.20819	.20894	.08218	.08500
5	.43150	.4446	.36029	.35342	.25026	.24566	.14080	.13956	.05069	.05153
100	.32610	.3346	.26247	.25587	.16950	.16507	.08395	.08228	.02376	.02329

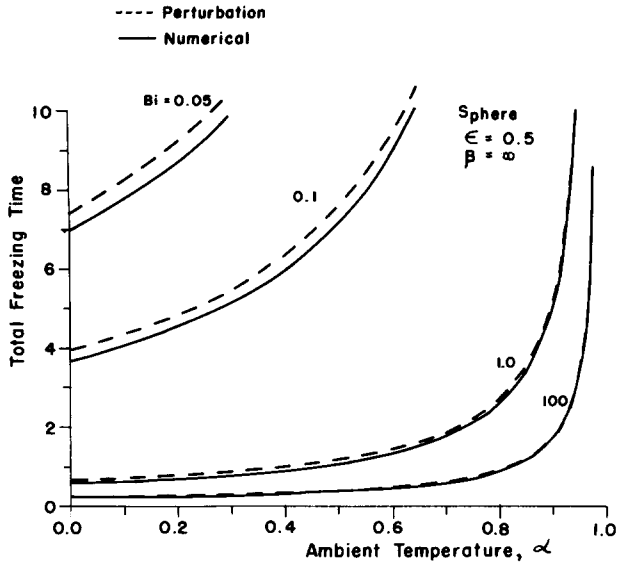

Figure 10 Time for complete freezing as a function of ambient temperature for various Bi (sphere: $\beta = \infty$)

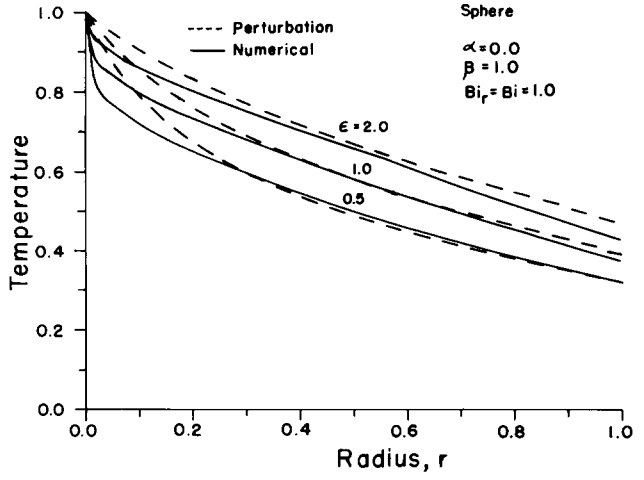

Figure 11 Temperature as a function of radial position for various Stefan numbers (sphere: $Bi = Bi_r = 1$)

moderate Biot numbers. Comparison of the numerical and the perturbation results for a Stefan number of 0.5 shows very good agreement. In general, the difference between the two results decreases with decreases in the Stefan number and increases in the Biot number. A change in the dimensionless ambient temperature does not noticeably affect the accuracy of the perturbation results.

Temperature profiles

The temperature profile computed from the perturbation analysis is compared with the numerical result in Figure 11. The result for the sphere is shown at $\alpha = 0.0$ and $\beta = 1.0$ ($Bi = Bi_r = 1.0$). The agreement is reasonable for larger dimensionless radii. However, the two results diverge in the vicinity of the center, with a maximum error of approximately 8%. The temperature profile for the cylindrical case is similar but is not presented here for space reasons. However, the perturbation results for both the sphere and the cylinder are compared with the numerically computed values. The results for two selected values of α are presented in Table 3.

Conclusion

Comparison of the two methods for solution of the inward solidification in radial systems suggests several conclusions. First, the perturbation method can provide accurate solutions for Stefan numbers below 0.5. As discussed—and depending on other parameters—reasonably accurate results are obtained even for values as high as $\varepsilon = 2.0$ (for water, $\varepsilon \approx 1.6$). Second, convective cooling is more effective, as expected, at smaller values of the dimensionless ambient temperature than is radiative cooling. At higher values of the ambient temperature, radiative cooling becomes significantly more important. Finally, the major advantage of the perturbation method remains its simplicity and significantly less required computational time (if any). The total required computational time for the perturbation method (which involved only numerical integration independent of the parameters of the problem) remained at least more than two orders of magnitude less than the computational time required for the numerical (enthalpy) method.

References

1 *Moving Boundary Problems*. D. G. Wilson, A. D. Solomon, and P. T. Boggs (eds.). Academic Press, New York, 1978
2 Rubinstein, L. I. *The Stefan Problem, Translation of Mathematical Monographs*, vol. 27. American Mathematical Society, Providence, RI, 1971
3 Crank, J. *Free and Moving Boundary Problems*. Clarendon Press, Oxford, 1984
4 *Moving Boundary Problems in Heat Flow and Diffusion*. J. R. Ockendon and W. R. Hodgkins (eds.). Clarendon Press, Oxford, 1975
5 Nayfeh, A. H. *Perturbation Methods*. Wiley-Interscience, New York, 1973
6 Kevorkain, J. and Cole, J. D. *Perturbation Methods in Applied Mathematics*. Springer-Verlag, New York, 1981
7 Aziz, A. and Na, T. Y. *Perturbation Methods in Heat Transfer*. Hemisphere, Washington, D.C., 1984
8 Rasmussen, H. and Christiansen, S. A perturbation solution for a two-dimensional annular electro-chemical problem. *J. Inst. Math. Applic.*, 1976a, **18**, 149–153

Table 3 Total freezing time calculated by the perturbation and numerical methods for different Bi_r and selected values of α ($\varepsilon = 0.5$, $\beta = 1.0$)

	Sphere				Cylinder			
	$\alpha = 0.2$		$\alpha = 0.6$		$\alpha = 0.2$		$\alpha = 0.6$	
Bi_r	Num.	Pert.	Num.	Pert.	Num.	Pert.	Num.	Pert
1	4.3025	4.5793	6.0015	6.3528	6.3675	6.6263	8.9225	9.2533
2	2.4235	2.5922	3.3700	3.5798	3.5685	3.7260	4.9905	5.1885
5	0.5845	0.6224	0.8495	0.8962	0.8480	0.8841	1.2470	1.2940
100	0.2746	0.2859	0.4876	0.5068	0.3913	0.4031	0.7082	0.7294

9 Rasmussen, M. and Christiansen, S. Numerical solutions for two-dimensional annular electrochemical machining problems. *J. Inst. Math. Applic.*, 1976b, **18**, 195–307

10 Duda, J. L. and Vrentas, J. S. Mathematical analysis of bubble dissolution. *AIChE Journal*, 1969a, **15**(3), 351–356

11 Duda, J. L. and Vrentas, J. S. Perturbation solutions of diffusion-controlled moving boundary problems. *Chem. Eng. Science*, 1969b, **24**, 261–470

12 Vrentas, J. S. and Shih, D. Perturbation solution of spherical moving boundary problems—I, Slow growth dissolution rates. *Chem. Eng. Science*, 1980a, **35**, 1687–1696

13 Vrentas, J. S. and Shih, D. Perturbation solution of spherical moving boundary—II, Rapid growth or dissolution rates. *Chem. Eng. Science*, 1980b, **35**, 1697–1705

14 Chahine, G. L. and Liu, H. L. Collective effects on the growth of vapour bubbles in a superheated liquid. *ASME J. Fluids Eng.*, 1984, **106**, 486–490

15 Weinbaum, S. and Jiji, L. M. Singular perturbation theory for melting or freezing in finite domains initially not at the fusion temperatures. *ASME J. Appl. Mech.*, 1977, **44**, 25–30

16 Jiji, L. M. and Weinbaum, S. Perturbations solutions for melting or freezing in annular regions initially not at the fusion temperature. *Int. J. Heat Mass Transfer*, 1978, **21**, 581–592

17 Goodling, J. S. and Khader, M. S. Inward solidifications with radiation–convection boundary conditions. *J. Heat Transfer*, 1974, **96**, 114–115

18 Pedroso, R. I. and Domoto, G. A. Inward spherical solidification—Solidification by the method of strained coordinates. *Int. J. Heat Mass Transfer*, 1973, **16**, 1037–1043

19 Milanez, L. F. and Boldrini, J. L. Perturbation solution for spherical solidification by convective cooling. *J. Thermophysics and Heat Transfer*, 1988, **2**, 88–91

20 Huang, C. L. and Shih, Y. P. A perturbation method for spherical and cylindrical solidification. *Chem. Eng. Sci.*, 1975, **30**, 897–906

21 Voller, V. R. and Cross, M. Estimating the solidification/melting times of cylindrically symmetric regions. *Int. J. Heat Mass Transfer*, 1981, **24**(9), 1457–1462

22 Voller, V. R. Implicit finite-difference solutions of the enthalpy formulation of Stefan problems. *IMA J. Num. Anal.*, 1985, **5**, 201–214